



Published in final edited form as:

Photochem Photobiol Sci. 2013 August ; 12(8): 1328–1340. doi:10.1039/c3pp25430e.

Excited state Proton-coupled electron transfer in 8-oxoG-C and 8-oxoG-A base pairs: A time dependent density functional theory (TD-DFT) study

Anil Kumar and Michael D. Sevilla

Department of Chemistry, Oakland University, Rochester, Michigan 48309, United States

Abstract

In a recent experiment, the repair efficiency of DNA thymine cyclobutane dimers ($T\langle\rangle T$) on UV excitation of 8-oxoG base paired either to C or A was reported. An electron transfer mechanism from an excited charge transfer state of 8-oxoG-C (or 8-oxoG-A) to $T\langle\rangle T$ was proposed and 8-oxoG-A was found to be 2 – 3 times more efficient than 8-oxoG-C in repair of $T\langle\rangle T$. Intra base pair proton transfer (PT) in charge transfer (CT) excited states of the base pairs was proposed to quench the excited state and prevent $T\langle\rangle T$ repair. In this work, we investigate this process with TD-DFT calculations of the excited states of 8-oxoG-C and 8-oxoG-A base pairs in the Watson-Crick and Hoogsteen base pairs using long-range corrected density functional, ω B97XD/6–31G* method. Our gas phase calculations showed that CT excited state ($^1\pi\pi^*(CT)$) of 8-oxoG-C appears at lower energy than the 8-oxoG-A. For 8-oxoG-C, TD-DFT calculations show the presence of a conical intersection (CI) between the lowest $^1\pi\pi^*(PT-CT)$ excited state and the ground state which likely deactivates the CT excited state via a proton-coupled electron transfer (PCET) mechanism. The $^1\pi\pi^*(PT-CT)$ excited state of 8-oxoG-A base pair lies at higher energy and its crossing with ground state is inhibited because of a high energy gap between $^1\pi\pi^*(PT-CT)$ excited state and ground state. Thus the gas phase calculations suggest the 8-oxoG-A would have longer excited state lifetimes. When the effect of solvation is included using the PCM model, both 8-oxoG-A and 8-oxoG-C show large energy gaps between the ground state and both the excited CT and PT-CT states and suggest little difference would be found between the two base pairs in repair of the $T\langle\rangle T$ lesion. However, in the FC region the solvent effect is greatly diminished owing to the slow dielectric response time and smaller gaps would be expected.

Keywords

8-oxo-7,8-dihydroguanine (8-oxoG); excited state; proton-coupled electron transfer; PCET; excited state electron-induced proton transfer; density functional; thymine dimer ($T\langle\rangle T$)

1. Introduction

DNA, the carrier of genetic information for all cellular forms of life, is susceptible to specific types of DNA damage from ultraviolet (UV) light. The major photoproducts on UV

radiation of cellular DNA are the cyclobutane pyrimidine dimers, such as, the thymine cyclobutane photodimer (T<>T) formed by the [2+2] cycloaddition of the stacked thymines.¹⁻⁶ Using femtosecond time-resolved infrared spectroscopy Schreier et al.⁶ showed the formation of cyclobutane dimers in the oligodeoxynucleotide (dT)₁₈ within ca. 1 picosecond after the UV excitation at 272 nm. In a very recent study, Pan et al.⁷ have determined the quantum yield for the formation of T<>T for a series of short DNA single-strand and base-paired hairpin structures possessing a single thymine-thymine step with flanking purines. These authors found that the quantum yield for the formation of T<>T photodimer was very strongly dependent upon the oxidation potential of the purines and decreasing in the order: hypoxanthine > adenine > guanine > deazaguanine.⁷ Mechanisms of repair of T<>T photodimers are of considerable interest^{3,8,9-18}. Studies have shown that both: (i) direct photoreversal^{3,8} and (ii) indirect photoreversal⁹⁻¹⁴ mechanisms are possible. We note that nucleotide excision repair (NER) is also a versatile repair pathway which involves enzymatic removal of the UV-induced cyclobutane pyrimidine dimers.¹⁶⁻¹⁸

Very recently, Nguyen and Burrows studied the photoreversal of damaged T<>T present in DNA duplexes containing 8-oxo-7,8-dihydroguanine (8-oxoG). In their experiment, they exposed the damaged DNA to UV light that electronically excited an 8-oxoG which was placed at different positions with respect to a T<>T in DNA and monitored the repair rates of the T<>T.¹²⁻¹⁴ The results found suggest that the T<>T repair via photoreversal supported a catalytic role played by 8-oxoG. The mechanism involved the transfer of an excess electron from the excited 8-oxoG to the T<>T. This resulted in the cleavage of the T<>T cyclobutane ring which is followed by back electron transfer to 8-oxoG^{•+} restoring the original 8-oxoG. The repair rate was found to depend on both the location of the 8-oxoG and on its base-pairing partner in the damaged DNA. When 8-oxoG paired with cytosine (8-oxoG-C) in the Watson-crick conformation the repair was 2 – 3 times slower than the 8-oxoG paired with adenine (8-oxoG_{syn}-A_{anti}) in a Hoogsteen base pair.^{13,14} To account for the slow repair rate of T<>T by the excited 8-oxoG-C base pair it was speculated that a fast deactivation of the CT excited state in 8-oxoG-C base pair occurred via a proton-coupled electron transfer (PCET) mechanism. However, for 8-oxoG_{syn}-A_{anti} deactivation of the CT excited state through PCET was suggested to be less effective than found for 8-oxoG-C because the repair efficiency of nearby T<>T was higher for 8-oxoG_{syn}-A_{anti} than for 8-oxoG-C. Such fast deactivation mechanisms have been shown to occur within a picosecond and non-radiative decay of CT excited states in several DNA base pairs (G-C, A-T and a model base pair) through a PCET mechanism has already been proposed in the literature.¹⁹⁻²⁵

8-oxoG is the most common oxidatively generated DNA damage caused by ionizing or UV radiation and usually results from •OH addition to guanine or nucleophilic addition of water to one-electron oxidized guanine.²⁶⁻²⁸ The mechanism of 8-oxoG formation in cellular DNA has been well documented recently by Cadet et al.^{29,30} In DNA, 8-oxoG base pairs with cytosine in the Watson-Crick hydrogen-bonded fashion and it can also base pair with adenine in the Hoogsteen base pair between 8-oxoG and adenine in which they adopt syn- and anti-conformations (8-oxoG_{syn}-A_{anti}) in duplex DNA.^{31,32}

The standard reduction (SR) potential for the oxidation of guanine is the lowest (1.3 V) of all four main DNA bases. This has important implications in DNA since guanine acts as a “hole” sink and protects other bases from damage by one-electron oxidation. The SR potential for oxidation of 8-oxoG is (0.7 V)¹⁴ and it is significantly lower than that of guanine. Thus, 8-oxoG is a far better “hole” scavenger than guanine in DNA.³³ While the excited states of the G-C base pair have been extensively studied by experiment and theory in order to better understand the deactivation mechanism of the charge transfer excited state^{19–25,34}, theoretical studies of the excited states of 8-oxoG-C or 8-oxoG-A base pairs have not been performed. The study of the excited states of 8-oxoG-C or 8-oxoG-A base pairs are of interest to understand the effect of possible charge transfer excited state formation on the T<>T repair process. In this work, we have investigated the excited states of 8-oxoG-C and 8-oxoG-A (8-oxoG_{syn}-A_{anti}) base pairs using long-range corrected time-dependent density functional theory (TD-DFT).

The organization of the present study is as follows: In section 2, the details of the ground and excited states calculations using the ω B97XD density functional is given. In section 3.1, the accuracy of the chosen functional for excited state calculation is compared with the available CC2 excited state energies of the G-C and A-T base pairs. The geometries of the ground and excited states, vertical excitation energies of 8-oxoG-C and 8-oxoG-A base pairs and the potential energy profile of the decay path of the 8-oxoG moiety in the two base pairs in the gas phase and in solution are discussed in sections 3.2 to 4.0. The outcome of the results is discussed in section 4.1.

2. Method of Calculations

In this work, we employed ω B97XD density functional recently developed by Chai and Head-Gordon.^{35,36} ω B97XD is a long-range corrected hybrid density functional with damped atom–atom dispersion corrections and has been found more reliable for the calculation of the dispersion as well as charge transfer (CT) excited states than results found using earlier density functionals.^{35,36} The initial geometry of 8-oxoG-C was generated by placing 8-oxoG and C monomers in the hydrogen-bonded Watson-Crick conformation while the geometry of 8-oxoG-A base pair was generated by placing the 8-oxoG and A in a Hoogsteen base pair. We attached methyl group to N₉ of guanine and adenine and N₁ of cytosine in the base pairs to mimic the effect of sugar ring as these sites are attached to the sugar ring in the DNA. The initial geometries of 8-oxoG-C and 8-oxoG-A thus generated were used for the optimization of their ground and excited states using the ω B97XD/6–31G* method. The ground state optimized geometries were used for calculation of the vertical excited states using the TD- ω B97XD/6–31G* method. The potential energy surface (PES) for proton transfer in the lowest CT excited state in the vertical and adiabatic states were calculated by choosing N1-H and N7-H bond lengths of 8-oxoG as reaction coordinate in 8-oxoG-C and 8-oxoG-A base pairs, respectively. For adiabatic calculations, at each chosen N-H bond length on the PES, the CT excited state was fully optimized by only constraining the corresponding bond length. The effect of solvation on the excited states of these base pairs are discussed in section 4.0. All the calculations were carried out using Gaussian 09 suite of programs.³⁷ JMOL³⁸ and GaussView³⁹ molecular modeling software were used to

draw molecular structures and molecular orbitals. In the text, we label highest occupied molecular orbital (HOMO) as H and the lowest unoccupied molecular orbital (LUMO) as L.

3. Results and Discussion

3.1 Suitability of the ω B97XD method for excited state calculation

To test the suitability of the ω B97XD/6–31G* method for the excited state calculations involving charge transfer excited states, we considered guanine(G)-cytosine(C) and adenine(A)-thymine(T) base pairs as test cases and calculated their singlet vertical excitation energies. The calculated excitation energies of G-C and A-T base pairs by the TD- ω B97XD/6–31G* method were compared with those calculated in references 40 and 41 using the Coupled Cluster singles and doubles (CC2) method^{42, 43}, see Tables 1 and 2.

For G-C base pair in C_s symmetry, the TD- ω B97XD/6–31G* method predicts the lowest two transitions (S_1 and S_2) as local excitations (LE) which are $^1\pi\pi^*$ in nature. The corresponding transition energies are 5.22 eV and 5.32 eV, respectively, and the oscillator strengths of these states are 0.0616 and 0.1036, see Table 1. The third transition (S_3) occurs at 5.45 eV with oscillator strength 0.0114 and it is also $^1\pi\pi^*$. It is due to the charge transfer from guanine to cytosine and designated as $G(\pi)\rightarrow C(\pi^*)$ in Table 1. The S_4 transition is a local excitation $C(n)\rightarrow C(\pi^*)$ with excitation energy 5.72 eV. The S_5 , S_6 , S_7 and S_8 transitions are local excitations and they are $^1\pi\pi^*$, $^1\pi\pi^*$, $^1n\pi^*$ and $^1n\pi^*$ types and occur at excitation energies 5.75 eV, 5.92 eV, 5.94 eV, 6.44 eV and 6.45 eV, respectively. The excited states of G-C base pair in C_s symmetry was studied by Yamazaki and Taketsugu⁴⁰ using the CC2/TZVP method. The CC2/TZVP method also predicts the lowest four transitions ($S_1 - S_4$) as $^1\pi\pi^*(LE)$, $^1\pi\pi^*(LE)$, $^1\pi\pi^*(CT)$ and $^1n\pi^*(LE)$ as calculated using the ω B97XD/6–31G* method. The CC2/TZVP calculated excitation energies are 4.88 eV, 5.06 eV, 5.23 eV and 5.49 eV, respectively, see Table 1. The CC2/TZVP method predicts S_5 and S_6 as local excitations $C(\pi)\rightarrow C(\pi^*)$, and $G(\pi)\rightarrow G(\pi^*)$ while ω B97XD/6–31G* method predicts these transitions as $G(\pi)\rightarrow G(\pi^*)$ and $C(\pi)\rightarrow C(\pi^*)$. The S_7 and S_8 transitions calculated by the CC2/TZVP method are $C(n)\rightarrow C(\pi^*)$ and $G(n)\rightarrow G(\pi^*)$. Thus, we see that the ω B97XD/6–31G* method predicts $S_1 - S_4$ transitions of G-C base pair in good agreement with those calculated by the CC2/TZVP method having a maximum difference of ca. 0.3 eV, see Table 1.

Using the CC2/TZVP method, Lange and Herbert⁴¹ calculated the six vertical singlet excitation energies of A-T base pair. The first transition (S_1) of A-T base pair, predicted by the CC2/TZVP method is a local excitation $T(n)\rightarrow T(\pi^*)$ and occurs at 4.94 eV, see Table 2. The $S_2 - S_4$ transitions are $^1\pi\pi^*$ type local excitations having excitation energies 5.21 eV, 5.40 eV and 5.47 eV, respectively, while the S_5 transition was predicted to be $A(n)\rightarrow A(\pi^*)$ type. The 6th transition (labeled as S_7 in Table 2) calculated by the CC2/TZVP method is a charge transfer excitation $A(\pi)\rightarrow T(\pi^*)$ and has excitation energy 6.04 eV. The ω B97XD/6–31G* calculated excitation energies of A-T base pair matched very well with those calculated by the CC2/TZVP method and have a maximum difference of ca. 0.3 eV except the first transition (S_1) for which the difference is ca. 0.4 eV. Thus, from these two test cases (G-C and A-T base pairs) we found that the ω B97XD /6–31G* method is suitable for the

excited state calculations having the charge transfer excitation and the calculated excitation energies are in excellent agreement with those calculated by the CC2/TZVP method.^{40,41}

3.2 Ground state geometry of 8-oxoG-C

The ground state (S_0) optimized geometry of 8-oxoG-C base pair in the Watson-Crick hydrogen-bonded conformation, calculated by the ω B97XD/6-31G* method, is presented in Figure 1(a). The atom numbering of 8-oxoG-C is shown in Table 3. The optimized structure is perfectly planar except the methyl groups attached to N9(G) and N1(C) sites. The bond angles surrounding atoms N2(G) and N4(C) constituting the NH_2 groups are 360 deg. which shows that NH_2 groups are planar in the base pair. The ω B97XD/6-31G* calculated distances between O6(G)---N4(C), N1(G)---N3(C) and N2(G)---O2(C) in 8-oxoG-C involved in hydrogen bonding are 2.81 Å, 2.91 Å and 2.90 Å, respectively. These calculated distances are in excellent agreement with those determined experimentally by X-ray³¹ and the corresponding distances are 2.85 Å, 2.95 Å and 2.84 Å, respectively.

3.3 Vertical excited states of 8-oxoG-C

The lowest seven ($S_1 - S_7$) vertical singlet excited states of 8-oxoG-C base pair calculated using the TD- ω B97XD/6-31G* method are presented in Table 3 and the molecular orbitals involved in the excitation are presented in Figure 2. The optimized ground state (S_0) geometry shown in Figure 1(a) is used for vertical excited state calculation. The TD- ω B97XD/6-31G* method predicts first transition (S_1) as $^1\pi\pi^*(\text{LE})$ localized on 8-oxoG with an excitation energy 4.79 eV and oscillator strength 0.1233. This transition (S_1) is dominated by $\text{H} \rightarrow \text{L}+2$ configuration, see Figure 2. The second transition (S_2) is a charge transfer excitation and $^1\pi\pi^*$ in nature and occurs at 5.17 eV with oscillator strength 0.0348. The charge transfer excitation (S_2) occurs between $\text{H} \rightarrow \text{L}$ and in this state 8-oxoG-C becomes 8-oxoG^{•+}-C^{•-}. The S_3 , S_4 and S_6 excitations are $^1\pi\pi^*(\text{LE})$ while S_5 and S_7 excitations are $^1n\pi^*(\text{LE})$, see Table 3. The S_3 , S_4 and S_6 excitations are dominated by $\text{H}-2 \rightarrow \text{L}$, $\text{H} \rightarrow \text{L}+3$ and $\text{H}-4 \rightarrow \text{L}$ and S_5 and S_7 excitations are dominated by $\text{H}-10 \rightarrow \text{L}$ and $\text{H}-5 \rightarrow \text{L}+2$, see Figure 2. In comparison to charge transfer excitation (5.45 eV) in G-C base pair (Table 1), the charge transfer excitation in 8-oxoG-C occurs at lower energy (5.17 eV; Table 3) and it is the second transition while in G-C base pair it is the third transition. The oscillator strength in both the systems are relatively low compared to the oscillator strength of the local $^1\pi\pi^*$ excitation. Thus, it is possible that these charge transfer states are populated by the nearby states having strong oscillator strengths and small energy difference, see Tables 1 and 2, respectively. Also, smaller charge transfer excitation of 8-oxoG-C than G-C is in accord with 8-oxoG being the site for primary oxidation instead of guanine in DNA. This is supported from the fact that the oxidation potential of 8-oxoG is ca. 0.6 V lower than G.¹²⁻¹⁴

3.4 Excited state geometries of 8-oxoG-C

The ω B97XD/6-31G* optimized structure of locally excited $^1\pi\pi^*(\text{LE})$ state (S_1) of 8-oxoG-C base pair is shown in Figure 1(b) and the optimized structure is planar. The hydrogen bonding distances between O6(G)---N4(C), N1(G)---N3(C) and N2(G)---O2(C) are 2.81 Å, 2.89 Å and 2.90 Å, respectively, which are similar to those calculated in the ground state, see Figure 1(a). Since the excitation is local to the 8-oxoG, there is no appreciable structural

change in the cytosine ring as the bond lengths are almost identical to the ground state structure, see Figures 1(a) and 1(b). However, as expected the 8-oxoG ring shows some structural change in compare to the ground state structure. In the excited state, the C4–C5 bond length increases by ca. 0.07 Å, C8–N7 bond length increases by ca. 0.03 Å and C8–N9 bond length decreases by 0.03 Å, respectively.

Interestingly, the full optimization of the charge transfer excited state $^1\pi\pi^*(CT)$ of 8-oxoG-C converges to the structure in which the N1 proton (H^+) of 8-oxoG transferred to the N3 of cytosine. To scan the adiabatic surface from the initial state to the final proton transferred state (see Figure 1(d)), we constrained the bond lengths of N1–H and N2–H of 8-oxoG to their ground state equilibrium bond lengths (see Figure 1(a)) and optimized the structure in the charge transfer $^1\pi\pi^*(CT)$ excited state using the TD- ω B97XD/6–31G* method. The resulting optimized structure is shown in Figure 1(c). Electron transfer from 8-oxoG to cytosine creates the charge transfer excited state. Thus, in the CT excited state 8-oxoG becomes a radical cation (8-oxoG $^{\bullet+}$) and cytosine becomes anion radical (C $^{\bullet-}$). On optimization of the excited 8-oxoG $^{\bullet+}$ -C $^{\bullet-}$ CT state, a large structural change occurs in the cytosine ring and creates a slightly non-planar overall structure. The NH₂ group of the cytosine becomes pyramidal (non-planar) and the angle surrounding the N4(C) is 331.7 deg. The non-planarity in the NH₂ group in the excited state has been found in earlier studies.^{40,44–46} The hydrogen bond distances between O6(G)---N4(C), N1(G)---N3(C) and N2(G)---O2(C) are 3.15 Å, 2.67 Å and 2.61 Å, respectively. In comparison to ground state, the N1(G)---N3(C) and N2(G)---O2(C) distances decrease by ca. 0.3 Å while the O6(G)---N4(C) distance substantially increases by ca. 0.3 Å. The C4–C5 bond of 8-oxoG lengthens by 0.04 Å, the N3–C4 and C4–C5 bonds of cytosine increase and decrease by 0.06 Å, respectively.

The optimized proton transferred charge transfer (PT-CT) excited state $^1\pi\pi^*$ of 8-oxoG-C is shown in Figure 1(d). In this PT-CT excited state the base pair 8-oxoG-C becomes a diradical, i.e. 8-oxoG(-H) $^{\bullet}$ -C(H) $^{\bullet}$. The structure is predicted to be planar by the ω B97XD/6–31G* method except for the NH₂ group of cytosine which shows small non-planarity (sum of angles surrounding N4 is 342 deg). The hydrogen bond distances O6(G)---N4(C), N1(G)---N3(C) and N2(G)---O2(C) are 3.08 Å, 2.96 Å and 2.86 Å, respectively. In comparison to ground state, the N3–C4 bond of cytosine increases by 0.07 Å while C4–C5 bond of cytosine decreases by 0.07 Å.

3.5 Excited state PCET reaction in 8-oxoG-C

The TD- ω B97XD/6–31G* calculated potential energy profile for intra base pair proton transfer from N1 of 8-oxoG to N3 of cytosine (see Table 3 for atom numbering) in the ground (S_0) and four lowest vertical excited states ($^1\pi\pi^*(LE)$, $^1\pi\pi^*(CT)$, $^1\pi\pi^*(LE)$ and $^1\pi\pi^*(LE)$) of 8-oxoG-C is shown in Figure 3. Along with the vertical excited state potential energy profile, we also present the optimized lowest $^1\pi\pi^*(LE)^{OPT}$ and $^1\pi\pi^*(CT)^{OPT}$ excited states calculated along the minimum-energy path for the proton transfer from N1(8-oxoG) and N3(C) in 8-oxoG-C using the same level of theory.

The potential energy profile, calculated in the vertical excited states, shows that the energy of the ground state (S_0) and three local excited states ($^1\pi\pi^*(LE)$) increase with increasing

N1-H distance, see Figure 3. However, the vertical charge transfer excited state ($^1\pi\pi^*(CT)$) decreases with increasing N1-H distance. Therefore it is dissociative in nature and crosses the lowest local excited state ($^1\pi\pi^*(LE)$) at N1-H distance around 1.25 Å, (see pink and green curves in Figure 3). Inspection of the vertical charge transfer excited state ($^1\pi\pi^*(CT)$; green curve) in Figure 3 shows that proton transfer from N1 of 8-oxoG to N3 of C is barrierless and exothermic in nature and predicts a shallow minimum around N1-H=1.8 Å. The energy gap between ground (S_0) and proton transferred $^1\pi\pi^*(CT)$ states at N1-H=1.8 Å is ca. 2.8 eV. This state ($^1\pi\pi^*(CT)$) is biradical in nature, i.e. 8-oxoG(-H) $^{\bullet}$ -C(H) $^{\bullet}$.

From Figure 3, it is evident that adiabatic lowest $^1\pi\pi^*(LE)^{OPT}$ (black curve) also shows bound nature as in the vertical state, i.e. the energy of this state ($^1\pi\pi^*(LE)^{OPT}$) rises with the increase of N1-H bond distance. The excited state geometry of $^1\pi\pi^*(LE)^{OPT}$ is given in Figure 1(b). The adiabatic charge transfer ($^1\pi\pi^*(CT)^{OPT}$; orange curve) is predicted to be the lowest excited state and in this state the structure is stabilized by a subsequent proton transfer from 8-oxoG to C without a substantial barrier. The TD- ω B97XD/6-31G* optimized geometry of the PT-CT excited state is shown in Figure 1(d). The optimization of this state shows that during proton transfer from 8-oxoG to C a small non-planarity in the structure takes place and after complete proton transfer the resulting structure (Figure 1(d)) becomes planar. The S_0' (ground state; lime color curve) is calculated using the corresponding $^1\pi\pi^*(CT)^{OPT}$ optimized excited state geometries. A crossing (conical intersection (CI)) is expected between the falling charge transfer $^1\pi\pi^*(CT)^{OPT}$ excited state and the continuous rising ground state S_0' curve. Such an intersection would efficiently deactivate the $^1\pi\pi^*(CT)^{OPT}$ back to the ground state.^{20,25} In the present calculation, we are not able to optimize the structure at the conical interaction because of the limitations of the TD-DFT method.⁴⁷ However, several studies pointed out that TD-DFT can provide reliable estimates of the geometry and the energy of minimum energy CI for single excitations.^{4,40,48} Our calculations show the presence of the stabilized charge transfer excited state ($^1\pi\pi^*(CT)^{OPT}$) at 0.6 eV from the ground state, see points enclosed by the broken circle in Figure 3. This relatively small energy difference clearly suggests that an efficient relaxation of the charge transfer excited state to the ground state is possible in 8-oxoG-C Watson-Crick conformation that is driven by an excited state PCET mechanism. Similar mechanism has been proposed in the literature for the G-C base pair^{19-21,23-25, 40} and in another model base pair.²² It is interesting to note that for G-C base pair in the Watson-Crick conformation, Sobolewski et al.²³ also calculated the energy gap (ca. 0.6 eV) between the proton transferred-charge transfer excited state and the ground state using the CC2 method as calculated for 8-oxoG-C in the present study.

3.6 Ground state geometry of 8-oxoG-A

The ground (S_0) state geometry of 8-oxoG-A base pair in Hoogsteen base pair arrangement, optimized by the ω B97XD/6-31G* method, is given in Figure 4(a). The Hoogsteen 8-oxoG-A base pair, in its ground state, has two hydrogen bonds between O6(8-oxoG)---N6(A) and N7(8-oxoG)---N1(A). The corresponding crystallographic distances are 3.06 Å and 2.70 Å, respectively.³² These hydrogen bond distances calculated by the ω B97XD/6-31G* method are 2.92 Å and 2.82 Å, respectively. The calculated structure adopts perfectly planar

structure except obviously for the hydrogens of the methyl groups at N9 sites of both the bases.

3.7 Vertical excited states of 8-oxoG-A

The nine lowest ($S_1 - S_9$) vertical excitation energies (E in eV), oscillator strength (f) and type of transition, calculated by the TD- ω B97XD/6-31G* level of theory for 8-oxoG-A, are presented in Table 4. Molecular orbitals involved in the excitations are shown in Figure 5. For 8-oxoG-A, the TD- ω B97XD/6-31G* method predicts eight transitions ($S_1 - S_6$, S_8 and S_9) as local excitations and S_7 as charge transfer. The S_1 and S_2 excitations are $^1\pi\pi^*(LE)$ with energies 4.61 eV and 5.44 eV and oscillator strengths 0.2128 and 0.0936, see Table 4. These transitions (S_1 and S_2) take place mainly between $H \rightarrow L$ and $H \rightarrow L+2$ molecular orbitals localized on 8-oxoG, see Figure 5. The S_3 , S_4 and S_5 excitations are $^1\pi\pi^*(LE)$, $^1\pi\pi^*(LE)$ and $^1n\pi^*(LE)$ and localized on adenine. The energies of these excitations ($S_3 - S_5$) are 5.47 eV, 5.57 eV and 5.66 eV, respectively. The S_6 excitation is $^1n\pi^*$ in nature and delocalized on A and 8-oxoG. The transition energy and oscillator strength for this excitation is 6.04 eV and 0.0003. The S_7 transition is a charge transfer excitation $^1\pi\pi^*(CT)$ with excitation energy 6.16 eV and oscillator strength 0.0016. This state (S_7) is dominated by $H \rightarrow L+1$ localized on 8-oxoG and adenine, see Figure 5. The $^1\pi\pi^*(CT)$ excited state of 8-oxoG-A lies ca. 1 eV above the $^1\pi\pi^*(CT)$ of 8-oxoG-C (Table 3). S_8 and S_9 transitions are $^1n\pi^*$ and $^1\pi\pi^*$ local excitations and occur at 6.19 eV and 6.56 eV with oscillator strength 0.0001 and 0.2895.

3.8 Excited state geometries of 8-oxoG-A

The PT-CT excited state geometry of 8-oxoG-A base pair in Hoogsteen base pair arrangement, optimized by the ω B97XD/6-31G* method, are given in Figures 4(b). The PT-CT excited ($^1\pi\pi^*(CT)$) state of 8-oxoG-A is biradical in nature (8-oxoG(-H) \cdot -A(H) \cdot). The geometry in this excited state was optimized by constraining the C2(A)-C8(oxoG)-C6(8-oxoG)-N6(A) dihedral angle to the ground state value (ca. 0 deg.) because during full optimization both the bases were tending to twist by more than 70 deg. and convergence could not be achieved. Further this motion would be hindered in a stacked DNA system. The TD- ω B97XD/6-31G* optimized geometry in this excited state shows large structural changes in the hydrogen bonding region. The O6(8-oxoG)---N6(A) and N7(8-oxoG)---N1(A) distances are appreciably increased by ca. 0.2 Å and ca. 0.3 Å in comparison to the corresponding ground state distances, see Figures 4(a) and (b). In the excited state, C4-C5, C5-C6 and C5-N7 bonds of 8-oxoG are slightly increased by 0.03 Å – 0.05 Å and N1-C2, C2-N3, N3-C4 and C4-C5 bonds in adenine are increased by 0.03 Å – 0.09 Å in comparison to the ground state distances.

3.9 Excited state PCET reaction in 8-oxoG-A

The potential energy profile of 8-oxoG-A base pair in the vertical excited state, considering the N7-H bond distance of 8-oxoG as the reaction coordinate, is shown in Figure 6. Figure 6 provides qualitative information about curve crossing as found for 8-oxoG-C in Figure 3.

From Figure 6, it is evident that the energy of the ground (S_0) state increases with the increase of N7-H bond distance of 8-oxoG in the base pair. The charge transfer excited state

($^1\pi\pi^*(CT)$) in this case shows a barrierless proton transfer from N7 of 8-oxoG to N1 of adenine. The energy of this state decreases with increasing N7-H bond distance and beyond 1.4 Å, the PT-CT excited ($^1\pi\pi^*(CT)$) state crosses the lowest $^1\pi\pi^*(LE)$ (pink curve in Figure 6) and becomes the lowest excited state and stabilized at N7-H=1.8 Å, see Figure 6. The energy gap at this point (N7-H=1.8 Å) with respect to the ground state is ca. 3.3 eV which is about 0.5 eV higher than the energy gap calculated for the PT-CT excited state in 8-oxoG-C pair, see Figure 3.

In Figure 7, we present the energy level diagram of the optimized PT-CT excited state ($^1\pi\pi^*(CT)^{OPT}$) of 8-oxoG-A base pair. From Figure 7, we see that the optimized PT-CT excited state ($^1\pi\pi^*(CT)^{OPT}$) of 8-oxoG-A lies ca. 1.2 eV above the ground state. This energy gap (1.2 eV) is quite large in comparison to the 8-oxoG-C base pair (0.6 eV), Figure 3. The present calculations are in close agreement with those concluded by Sobolewski et al.²³ Using the CC2 method Sobolewski et al.²³ showed that for G-C base pair in specific hydrogen bonding conformations, the crossing between $^1\pi\pi^*(CT)$ and ground state of G-C pair in the Watson-Crick conformation occurs at smaller energy (0.6 eV) than the other conformations.

4.0 Effect of solvation on excited state PCET reactions in 8-oxoG-C and 8-oxoG-A

The effect of solvation on the excited state PCET reactions in 8-oxoG-C and 8-oxoG-A base pairs has been incorporated through the use of the polarizable continuum model (PCM) using the integral equation formalism (IEF). The ground state geometries of 8-oxoG-C and 8-oxoG-A base pairs in solution were optimized using the PCM- ω B97XD/6-31G* method and their vertical excited states were calculated. The calculated vertical excitation energies are presented in Table 5. From Table 5, it is evident that local excited states energies are not much affected by the solvation on comparison to their gas phase energies, see Tables 3 and 4. The CT excited state of 8-oxoG-C in solution is predicted to be 4th transition (S_4) with energy 5.93 eV (Table 5) while in the gas phase it is the 2nd transition (S_2) with energy 5.17 eV (Table 3). The CT excited states energies of oxoG-A in solution and in the gas phase are 6.03 eV and 6.16 eV, respectively, see Tables 4 and 5.

The potential energy profile of solvated 8-oxoG-C and 8-oxoG-A base pairs in the vertical excited states are shown in Figures 8 and 9. For 8-oxoG-C base pair, the ground state (S_0) energy in solution increases with the increase of the N1-H bond distance of 8-oxoG, see Figure 8. The energy of the $^1\pi\pi^*(CT)$ excited state decreases with increasing N1-H bond distance and after (N1-H = 1.4 Å) it becomes the lowest excited state as found in the gas phase. The potential energy profile of the solvated 8-oxoG-A base pair is similar to the 8-oxoG-C base pair. The $^1\pi\pi^*(CT)$ in 8-oxoG-A becomes the lowest after N7-H = 1.4 Å. The energy difference between ground state and the lowest PT-CT excited state at 1.8 Å in 8-oxoG-C and 8-oxoG-A base pairs are 4.56 eV and 4.28 eV, respectively, see Figures 8 and 9.

The energy level diagram of the optimized PT-CT excited state ($^1\pi\pi^*(CT)^{OPT}$) of 8-oxoG-C and 8-oxoG-A base pairs calculated in different dielectric constants ($\epsilon = 78.4$ (water); $\epsilon =$

4.0 and $\epsilon = 1.0$ gas phase) in planar conformation are shown in Figures 10 and 11. The dielectric constant $\epsilon = 4.0$ represents the dielectric within DNA.²⁴ From these figures, it is evident that PT in the CT excited state is highly influenced by the dielectric constant of the surroundings. In water solution ($\epsilon = 78.4$) the energy gap between the ground state and PT-CT excited state is large (ca. 3.3 eV) in both the cases and this gap decreases with decrease in the dielectrics of the medium. Recently, the excited state decay of C-C base pair in Watson-Crick conformation in chloroform (CHCl_3) have been studied using the broad-band transient absorption spectroscopy and quantum mechanical calculations using PCM-TD-DFT by Biemann et al.⁴⁹ This study also shows a large energy gap between the ground and PT-CT excited states and proposed the involvement of an intrastrand excimer for fast fluorescence decay. Similar conclusions were drawn for A-T base pair using the PCM-TD-DFT method by Improta and coworkers.⁵⁰ Markovitsi⁵¹ and Kohler⁵² groups also support the excited states decay via intrastrand exciplexes in G-C DNA duplexes.

Schwalb and Temps²⁴ reported the femtosecond time resolved experiment on G-C base pair in solution (CHCl_3) and proposed the fast deactivation of G-C base pair through excited state PCET mechanism. The fluorescence lifetime of G-C pair in the Watson-Crick conformation reported to be 0.355 picoseconds by Schwalb and Temps²⁴ in agreement with QM/MM molecular dynamics simulations (0.29 ± 0.05).²⁵ Recently, Kohler and coworkers⁵³ reported the fast deactivation in G-C oligonucleotide through an excited state PCET with the possibility of the formation of an intrastrand exciplex state. The recent electron spin resonance (ESR) experiment of one-electron oxidized G-C DNA oligomers confirms the interbase proton transfer from $\text{G}^{•+}$ to C at 77 K.⁵⁴ This was further supported by the theory by incorporating explicit water molecules constituting the first hydration layer around one-electron oxidized G-C base pair.⁵⁵ Marwick and Doltsinis used nonadiabatic molecular dynamics simulations to calculate excited-state lifetimes of the G-C Watson-Crick pair in the gas phase and in aqueous solution and an excited state coupled proton-electron transfer from G to C along the central hydrogen bond is observed upon excitation of the $\pi\pi^*$ state initially localized on G.²⁵ Thus, it seems that excited state proton transfer in solution depends on several factors such as the dynamics of the solute-solvent interaction, including the hydrogen bonding between water and solute (first hydration layer) and location of the counter ions in DNA which are absent in the solvation model. The fast excited state deactivation in DNA is possibly mediated through exciplex states with significant CT character which enable proton transfer across base pairs as pointed out by Kohler and coworkers.⁵³

4.1 Conclusions

This theoretical study was stimulated by the recent experiments of Nguyen and Burrows.¹²⁻¹⁴ These workers found that 8-oxoG-A mismatch base pair in DNA is 2 – 3 times more efficient than the 8-oxoG-C base pair in repair of the T<>T dimer. Our gas phase calculations suggest that the CT-excited state would rapidly decay via a barrierless transfer of the N1-H proton of 8-oxoG to N3 of cytosine, see Figure 3. The relatively small energy gap (ca. 0.6 eV) in the gas phase between ground and S_1 state suggests a crossing between these two states (conical intersection) that rapidly deactivates the $^1\pi\pi^*(\text{CT})$ excited state as calculated for G-C base pair using multiconfigurational ab initio calculations and QM/MM

molecular dynamics simulations.^{20,25} On the other hand, the $^1\pi\pi^*(CT)$ excited state of 8-oxoG-A occurs at higher energy than the 8-oxoG-C pair. The larger energy gap (ca. 1.2 eV) between ground and excited state (Figure 7) would also inhibit the deactivation process through the PCET mechanism and enhance the life time of this state.

When the surrounding medium is included we find the situation changes. The excited PT-CT state in 8-oxoG-C and 8-oxoG-A base pairs lies at much higher energies from the ground state for water (3.3 eV for both at $\epsilon = 78.4$) and for DNA (2.6 eV for 8-oxoG-C and 2.9 eV for 8-oxoG-A at $\epsilon = 4$) than found for the gas phase calculations (0.6 eV for 8-oxoG-C and 1.2 eV for 8-oxoG-A at $\epsilon = 1$). These large energy gaps in solution lower the probability that fast deactivation through PCET as found in the gas phase for 8-oxoG-C occurs. Since both 8-oxoG-A and 8-oxoG-C show large energy gaps between the ground state and both the excited CT and PT-CT states we would expect longer lifetimes for both and little difference between the two base pairs in repair of the T \leftrightarrow T lesion. We note that the PCM-TDDFT highly destabilizes the CT excited state and would appear to prohibit the mechanism proposed by Burrows and coworkers.¹⁴ However, it is important to note that in the FC region, only the electronic cloud of the surrounding medium (solvent) responds so that the initial dielectric constant(ϵ) of the medium is about 2.¹⁵ Thus in the Franck-Condon (FC) region the solvent effect is minimized and solvent has a relatively small effect on the CT transitions and subsequent fast deactivation processes if they are short with respect to the dielectric response time (ca. 20 ps).

Deactivation in these solvated systems could result from one of the other mechanisms discussed in section 4.0. For example, formation of an intrastrand excimer could lead to either fast fluorescence decay or a deactivation process through exciplex states as suggested by several groups.^{49–52} The possibility of significant CT character in the exciplex that would enable proton transfer across base pairs has been suggested.⁵³ Such a PCET mechanism in excited states has been suggested by several workers,^{24,25,53} however, a number of other recent works argue against this.^{49–52}

Acknowledgments

This work was supported by the NIH NCI under Grant No. R01CA045424, and computational studies were supported by a computational facilities Grant, NSF CHE-0722689.

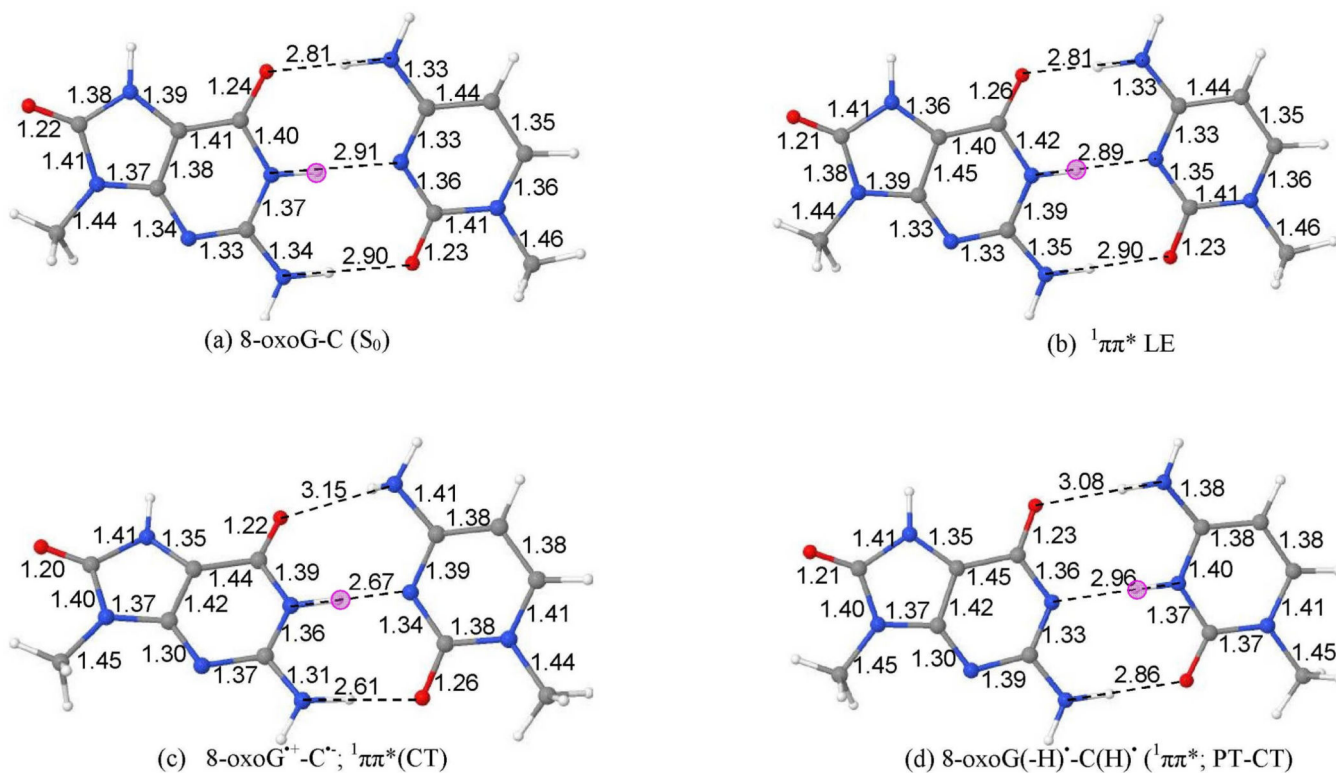
References

1. Beukers R, Berends W. Isolation and identification of the irradiation product of thymine. *Biochim. Biophys. Acta.* 1960; 41:550–551. [PubMed: 13800233]
2. Taylor JS. Unraveling the molecular pathway from sunlight to skin cancer. *Acc. Chem. Res.* 1994; 27:76–82.
3. Holman MR, Ito T, Rokita SE. Self-repair of thymine dimer in duplex DNA. *J. Am. Chem. Soc.* 2007; 129:6–7. [PubMed: 17199261]
4. Banyasz A, Douki T, Improta R, Gustavsson T, Onidas D, Vayá I, Perron M, Markovitsi D. Electronic excited states responsible for dimer formation upon UV absorption directly by thymine strands: Joint experimental and theoretical study. *J. Am. Chem. Soc.* 2012; 134:14834–14845. [PubMed: 22894169]

5. Schreier WJ, Kubon J, Regner N, Haiser K, Schrader TE, Zinth W, Clivio P, Gilch P. Thymine dimerization in DNA model systems: Cyclobutane photolesion is predominantly formed via the singlet channel. *J. Am. Chem. Soc.* 2009; 131:5038–5039. [PubMed: 19309140]
6. Schreier WJ, Schrader TE, Koller FO, Gilch P, Crespo-Hernández CE, Swaminathan VN, Carell T, Zinth W, Kohler B. Thymine dimerization in DNA is an ultrafast photoreaction. *Science*. 2007; 315:625–629. [PubMed: 17272716]
7. Pan Z, Hariharan M, Arkin JD, Jalilov AS, McCullagh M, Schatz GC, Lewis FD. Electron donor acceptor interactions with flanking purines influence the efficiency of thymine photodimerization. *J. Am. Chem. Soc.* 2011; 133:20793–20798. [PubMed: 22032333]
8. Johns HE, Rapaport SA, Delbrück M. Photochemistry of thymine dimers. *J. Mol. Biol.* 1962; 4:104–114. [PubMed: 14451976]
9. Kao YT, Saxena C, Wang L, Sancar A, Zhong D. Direct observation of thymine dimer repair in DNA by photolyase. *Proc. Natl. Acad. Sci U.S.A.* 2005; 102:16128–16132. [PubMed: 16169906]
10. Heil K, Pearson D, Carell T. Chemical investigation of light induced DNA bipyrimidine damage and repair. *Chem. Soc. Rev.* 2011; 40:4271–4278. [PubMed: 21076781]
11. Pan Z, Chen J, Schreier WJ, Kohler B, Lewis FD. Thymine dimer photoreversal in purine-containing trinucleotides. *J. Phys. Chem. B.* 2012; 116:698–704. [PubMed: 22103806]
12. Nguyen KV, Burrows CJ. Photorepair of cyclobutane pyrimidine dimers by 8-oxopurine nucleosides. *J. Phys. Org. Chem.* 2012; 25:574–577.
13. Nguyen KV, Burrows CJ. A prebiotic role for 8-oxoguanosine as a flavin mimic in pyrimidine dimer photorepair. *J. Am. Chem. Soc.* 2011; 133:14586–14589. [PubMed: 21877686]
14. Nguyen KV, Burrows CJ. Whence flavins? Redox-active ribonucleotides link metabolism and genome repair to the RNA world. *Acc. Chem. Res.* 2012; 45:2151–2159. [PubMed: 23054469]
15. Anusiewicz I, Wierszcz I, Skurski P, Simons J. Mechanism for repair of thymine dimers by photoexcitation of proximal 8-oxo-7,8-dihydroguanine. *J. Phys. Chem. A.* 2013; 117:1240–1253. [PubMed: 22894719]
16. van der Wees C, Jansen J, Vrieling H, van der Laarse A, Van Zeeland A, Mullenders L. Nucleotide excision repair in differentiated cells. *Mutat. Res.* 2007; 614:16–23. [PubMed: 16879838]
17. Friedberg, EC.; Walker, GC.; Siede, W.; Wood, RD.; Schultz, RA.; Ellenberger, T. DNA repair and mutagenesis. Washington, DC, USA: ASM Press; 2006.
18. Cadet J, Mouret S, Ravanat J-L, Douki T. Photoinduced damage to cellular DNA: Direct and photosensitized reactions. *Photochem. Photobiol.* 2012; 88:1048–1065. [PubMed: 22780837]
19. Kumar A, Sevilla MD. Proton-coupled electron transfer in DNA on formation of radiation-produced ion radicals. *Chem. Rev.* 2010; 110:7002–7023. [PubMed: 20443634]
20. Groenhof G, Schäfer LV, Boggio-Pasqua M, Goette M, Grubmüller H, Robb MA. Ultrafast deactivation of an excited cytosine-guanine base pair in DNA. *J. Am. Chem. Soc.* 2007; 129:6812–6819. [PubMed: 17488008]
21. Perun S, Sobolewski AL, Domcke W. Role of electron-driven proton-transfer processes in the excited-state deactivation of the adenine-thymine base pair. *J. Phys. Chem. A.* 2006; 110:9031–9038. [PubMed: 16854013]
22. Schultz T, Samoylova E, Radloff W, Hertel IV, Sobolewski AL, Domcke W. Efficient deactivation of a model base pair via excited-state hydrogen transfer. *Science*. 2004; 306:1765–1768. [PubMed: 15576616]
23. Sobolewski AL, Domcke W, Hättig C. Tautomeric selectivity of the excited-state lifetime of guanine cytosine base pairs: The role of electron-driven proton-transfer processes. *Proc. Natl. Acad. Sci U.S.A.* 2005; 102:17903–17906. [PubMed: 16330778]
24. Schwalb NK, Temps F. Ultrafast electronic relaxation in guanosine is promoted by hydrogen bonding with cytidine. *J. Am. Chem. Soc.* 2007; 129:9272–9273. [PubMed: 17622153]
25. Marwick PRL, Doltsinis NL. Ultrafast repair of irradiated DNA: Nonadiabatic ab initio simulations of the guanine-cytosine photocycle. *J. Chem. Phys.* 2007; 126:175102–175106. [PubMed: 17492887]
26. Shukla LI, Adhikary A, Pazdro R, Becker D, Sevilla MD. Formation of 8-oxo-7,8-dihydroguanine-radicals in γ -irradiated DNA by multiple one-electron oxidations. *Nucleic Acids Res.* 2004; 32:6565–6574. [PubMed: 15601999]

27. Steenken S, Jovanovic SV, Bietti M, Bernhard K. The trap depth (in DNA) of 8-Oxo-7,8-dihydro-2'-deoxyguanosine as derived from electron-transfer equilibria in aqueous solution. *J. Am. Chem. Soc.* 2000; 122:2373–2374.
28. Kasai H, Yamaizumi Z, Berger M, Cadet J. Photosensitized formation of 7,8-dihydro-8-oxo-2'-deoxyguanosine (8-Hydroxy-2'-deoxyguanosine) in DNA by riboflavin: A non singlet oxygen mediated reaction. *J. Am. Chem. Soc.* 1992; 114:9692–9694.
29. Cadet J, Douki T, Ravanat J-L. Oxidatively generated damage to the guanine moiety of DNA: Mechanistic aspects and formation in cells. *Acc. Chem. Res.* 2008; 41:1075–1083. [PubMed: 18666785]
30. Cadet J, Douki T, Ravanat J-L. Oxidatively generated base damage to cellular DNA. *Free Radic. Biol. Med.* 2010; 49:9–21. [PubMed: 20363317]
31. Lipscomb LA, Peek ME, Morningstar ML, Verghis SM, Miller EM, Rich A, Essigmann JM, Williams LD. X-ray structure of a DNA decamer containing 7,8-dihydro-8-oxoguanine. *Proc. Natl. Acad. Sci USA.* 1995; 92:719–723. [PubMed: 7846041]
32. McAuley-Hecht KE, Leonard GA, Gibson NJ, Thomson JB, Watson WP, Hunter WN, Brown Tom. Crystal structure of a DNA duplex containing 8-hydroxydeoxyguanine-adenine base pairs. *Biochemistry.* 1994; 33:10266–10270. [PubMed: 8068665]
33. Cai Z, Sevilla MD. Electron and hole transfer from DNA base radicals to oxidized product of guanine in DNA. *Radiat. Res.* 2003; 159:411–419. [PubMed: 12600244]
34. Crespo-Hernández CE, Cohen B, Hare PM, Kohler B. Ultrafast excited-state dynamics in nucleic acids. *Chem. Rev.* 2004; 104:1977–2019. [PubMed: 15080719]
35. Chai J-D, Head-Gordon M. Long-range corrected hybrid density functionals with damped atom–atom dispersion corrections. *Phys. Chem. Chem. Phys.* 2008; 10:6615–6620. [PubMed: 18989472]
36. Chai J-D, Head-Gordon M. Systematic optimization of long-range corrected hybrid density functionals. *J. Chem. Phys.* 2008; 128:084106. [PubMed: 18315032]
37. Frisch, MJ.; Trucks, GW.; Schlegel, HB.; Scuseria, GE.; Robb, MA.; Cheeseman, JR.; Scalmani, G.; Barone, V.; Mennucci, B.; Petersson, GA.; Nakatsuji, H.; Caricato, M.; Li, X.; Hratchian, HP.; Izmaylov, AF.; Bloino, J.; Zheng, G.; Sonnenberg, JL.; Hada, M.; Ehara, M.; Toyota, K.; Fukuda, R.; Hasegawa, J.; Ishida, M.; Nakajima, T.; Honda, Y.; Kitao, O.; Nakai, H.; Vreven, T.; Montgomery, JA., Jr; Peralta, JE.; Ogliaro, F.; Bearpark, M.; Heyd, JJ.; Brothers, E.; Kudin, KN.; Staroverov, VN.; Keith, T.; Kobayashi, R.; Normand, J.; Raghavachari, K.; Rendell, A.; Burant, JC.; Iyengar, SS.; Tomasi, J.; Cossi, M.; Rega, N.; Millam, JM.; Klene, M.; Knox, JE.; Cross, JB.; Bakken, V.; Adamo, C.; Jaramillo, J.; Gomperts, R.; Stratmann, RE.; Yazyev, O.; Austin, AJ.; Cammi, R.; Pomelli, C.; Ochterski, JW.; Martin, RL.; Morokuma, K.; Zakrzewski, VG.; Voth, GA.; Salvador, P.; Dannenberg, JJ.; Dapprich, S.; Daniels, AD.; Farkas, O.; Foresman, JB.; Ortiz, JV.; Cioslowski, J.; Fox, DJ. Wallingford CT: Gaussian, Inc.; 2010.
38. Jmol, An Open-Source Java Viewer for Chemical Structures in 3D. 2004 see <http://jmol.sourceforge.net>.
39. GaussView. Pittsburgh, PA: Gaussian, Inc.; 2003.
40. Yamazaki S, Taketsugu T. Photoreaction channels of the guanine–cytosine base pair explored by long-range corrected TDDFT calculations. *Phys. Chem. Chem. Phys.* 2012; 14:8866–8877. [PubMed: 22596076]
41. Lange AW, Herbert JM. Both intra- and interstrand charge-transfer excited states in aqueous B-DNA are present at energies comparable to, or just above, the $^1\pi\pi^*$ excitonic bright states. *J. Am. Chem. Soc.* 2009; 131:3913–3922. [PubMed: 19292489]
42. Hättig C, Weigend F. CC2 excitation energy calculations on large molecules using the resolution of the identity approximation. *J. Chem. Phys.* 2000; 113:5154–5161.
43. Christiansen O, Koch H, Jorgensen P. The second-order approximate coupled cluster singles and doubles model CC2. *Chem. Phys. Lett.* 1995; 243:409–418.
44. Shukla MK, Mishra PC. A gas phase ab initio excited state geometry optimization study of thymine, cytosine and uracil. *Chem. Phys.* 1999; 240:319–329.
45. Shukla MK, Mishra SK, Kumar A, Mishra PC. An ab initio study of excited states of guanine in the gas phase and aqueous media: Electronic transitions and mechanism of spectral oscillations. *J. Comp. Chem.* 2000; 21:826–846.

46. Shukla MK, Leszczynski J. Electronic spectra, excited state structures and interactions of nucleic acid bases and base assemblies: A review. *J. Biomol. Struct. Dyn.* 2007; 25:93–118. [PubMed: 17676942]
47. Levine BG, Ko C, Quenneville J, Marti ez TJ. Conical intersections and double excitations in time-dependent density functional theory. *Mol. Phys.* 2006; 104:1039–1051.
48. Tapavicza E, Tavernelli I, Rothlisberger U, Filippi C, Casida ME. Mixed time-dependent density-functional theory/classical trajectory surface hopping study of oxirane photochemistry. *J. Chem. Phys.* 2008; 129:124108. [PubMed: 19045007]
49. Biemann L, Kovalenko SA, Kleinermanns K, Mahrwald R, Markert M, Improta R. Excited state proton transfer is not involved in the ultrafast deactivation of guanine cytosine pair in solution. *J. Am. Chem. Soc.* 2011; 133:19664–19667. [PubMed: 22074113]
50. Dargiewicz M, Biczysko M, Improta R, Barone V. Solvent effects on electron-driven proton-transfer processes: adenine–thymine base pairs. *Phys. Chem. Chem. Phys.* 2012; 14:8981–8989. [PubMed: 22398748]
51. Miannay F-A, Bányász A, Gustavsson T, Markovitsi D. Ultrafast excited-state deactivation and energy transfer in guanine-cytosine DNA double helices. *J. Am. Chem. Soc.* 2007; 129:14574–14575. [PubMed: 17983238]
52. Crespo-Hernández CE, de La Harpe K, Kohler B. Ground-state recovery following UV excitation is much slower in G-C-DNA duplexes and hairpins than in mononucleotides. *J. Am. Chem. Soc.* 2008; 130:10844–10845. [PubMed: 18646753]
53. de La Harpe K, Crespo-Hernández CE, Kohler B. Deuterium isotope effect on excited-state dynamics in an alternating GC oligonucleotide. *J. Am. Chem. Soc.* 2009; 131:17557–17559. [PubMed: 19950991]
54. Adhikary A, Khanduri D, Sevilla MD. Direct observation of the hole protonation state and hole localization site in DNA-oligomers. *J. Am. Chem. Soc.* 2009; 131:8614–8619. [PubMed: 19469533]
55. Kumar A, Sevilla MD. Influence of hydration on proton transfer in the guanine-cytosine radical cation ($G^{*+}-C$) base pair: A density functional theory study. *J. Phys. Chem. B.* 2009; 113:11359–11361. [PubMed: 19485319]

**Figure 1.**

The ω B97XD/6-31G* calculated optimized structures of 8-oxoG-C base pair in (a) ground state (S_0), (b) $^1\pi\pi^*$ LE, (c) 8-oxoG⁺-C⁻; $^1\pi\pi^*$ (CT) (N1-H and N2-H in 8-oxoG were constrained during optimization) and (d) PT-CT 8-oxoG(-H)⁻-C(H)⁺; ($^1\pi\pi^*$; PT-CT)). The pink circle shows the location of proton in the base pairs.

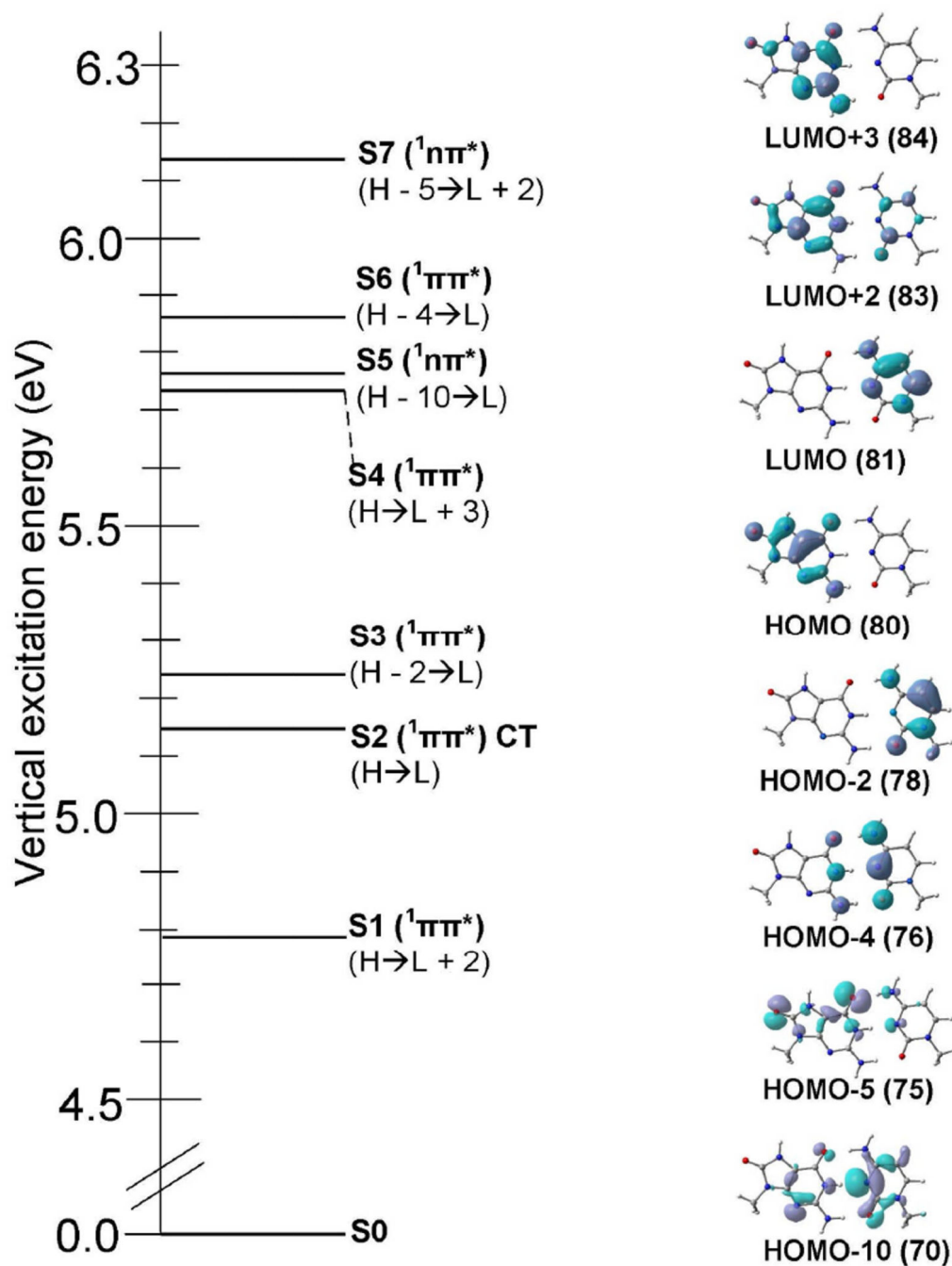


Figure 2.

Vertical excitation energy in eV of 8-oxoG-C base pair obtained using the TD- ω B97XD/6-31G* method ($\epsilon = 1$). The nature of the transition and molecular orbitals involved in the excitation (S1 – S7) are also given. H= HOMO (highest occupied molecular orbital); L= LUMO (lowest unoccupied molecular orbital). For details, see Table 3.

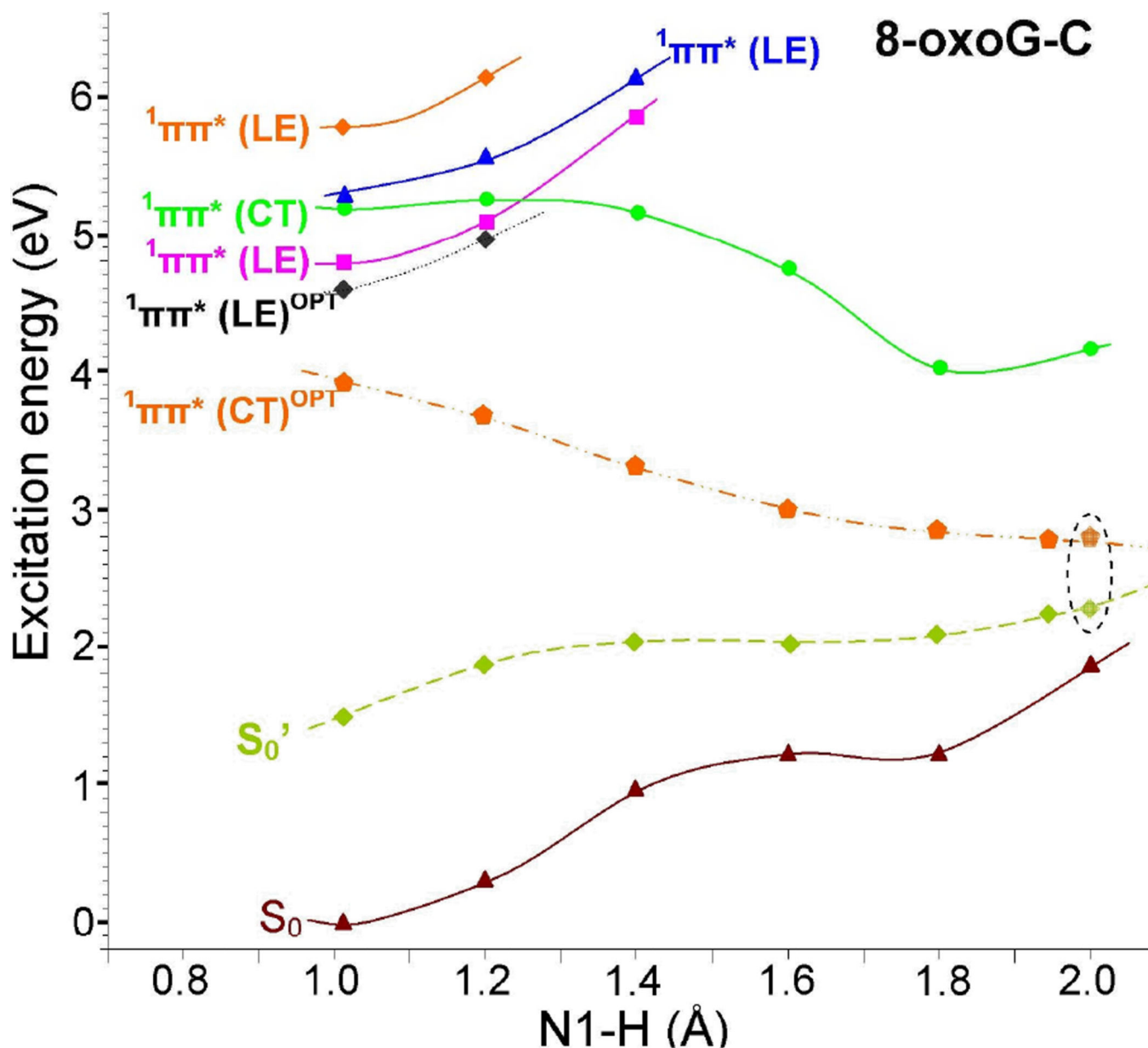


Figure 3. Potential energy surface (PES) profile of the ground (S_0), the three lowest $^1\pi\pi^*(LE)$ and the lowest $^1\pi\pi^*(CT)$ excited states of 8-oxoG-C base pair calculated using the TD- ω B97XD/6-31G* method ($\epsilon = 1$) considering N1-H of 8-oxoG as a reaction coordinate, see Figure 1(a) and Table 3. The optimized lowest $^1\pi\pi^*(CT)^{OPT}$ state is also shown. The ground state (S_0') surface is obtained from a single point energy calculation using the corresponding optimized geometries of $^1\pi\pi^*(CT)^{OPT}$ states. All the energies were calculated using the energy of the optimized ground state of 8-oxoG-C base pair, shown in Figure 1(a), as reference. All states are vertical except for those labeled OPT which are adiabatic.

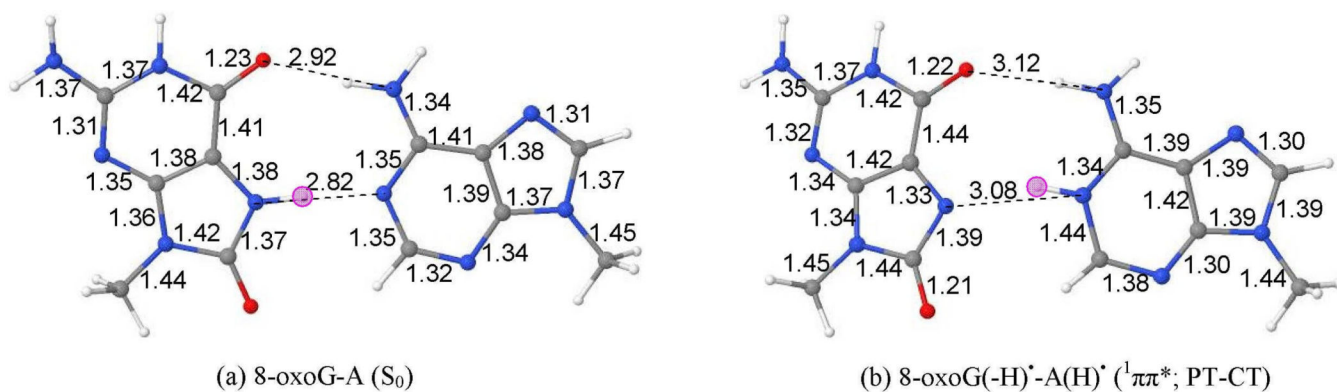


Figure 4. ω B97XD/6-31G* calculated optimized structures of 8-oxoG-A base pair in (a) ground state (S_0) and (b) proton transferred 8-oxoG(-H)⁻-A(H)⁺; ($^1\pi\pi^*$ (CT)). Pink circle in (a) and (b) shows the location of transferring proton.

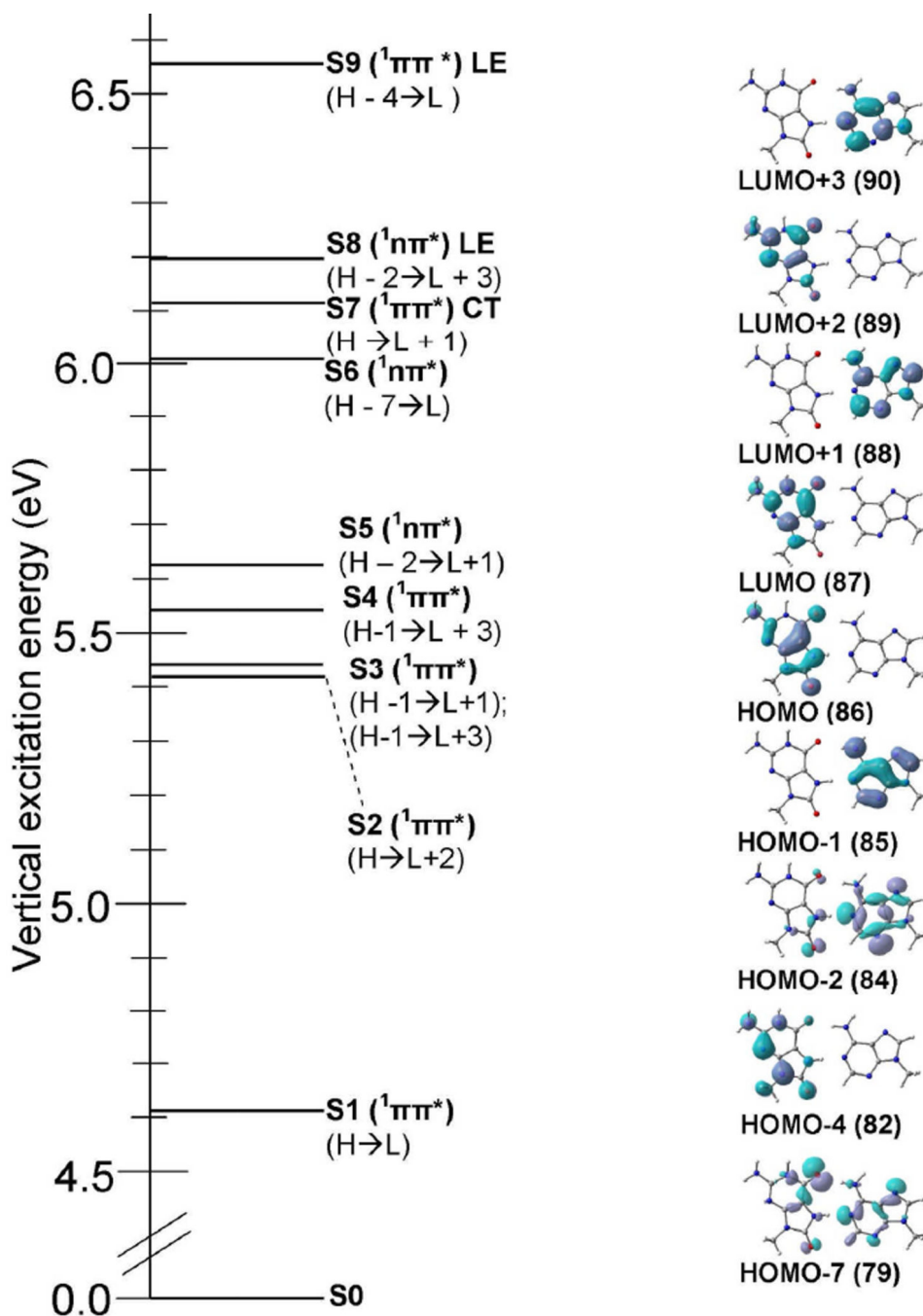


Figure 5. Vertical excitation energy in eV of 8-oxoG-A base pair obtained using the TD- ω B97XD/6-31G* method ($\epsilon = 1$). The nature of the transition and molecular orbitals involved in the excitation (S1 – S9) are also given. For details, see Table 3.

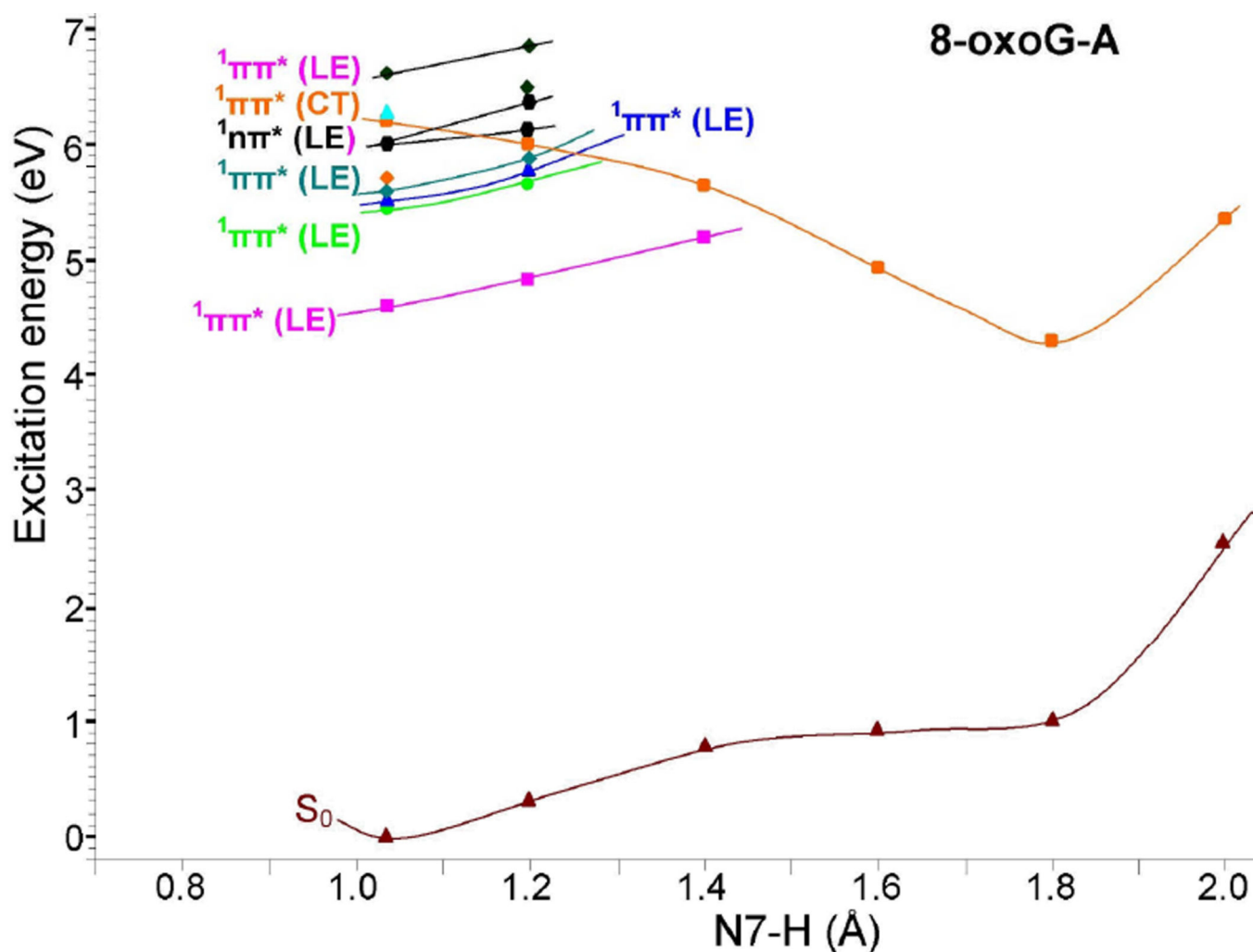


Figure 6. Vertical potential energy surface (PES) profile of the ground (S_0), $^1\pi\pi^*(LE)$, $^1n\pi^*(LE)$ and the lowest $^1\pi\pi^*(CT)$ excited states of 8-oxoG-A base pair calculated using the TD- ω B97XD/6-31G* method ($\epsilon = 1$) considering N7-H of 8-oxoG as a reaction coordinate, see Figure 4(a) and Table 4. All the energies were calculated using the energy of the optimized ground state of 8-oxoG-A base pair, shown in Figure 4(a), as reference.

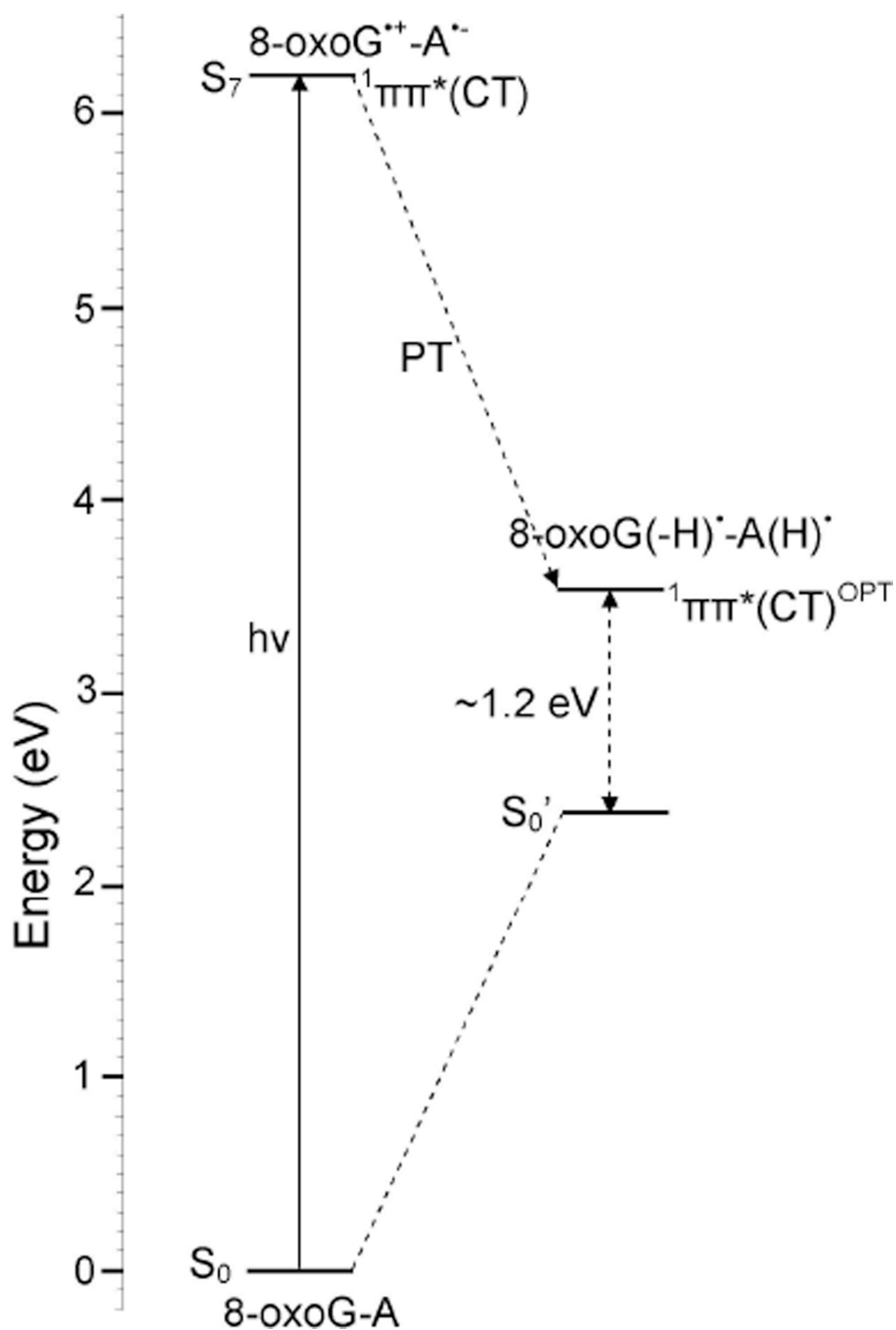


Figure 7. Energy level diagram of ${}^1\pi\pi^*(CT)$ excited states of 8-oxoG-A base pair along with the optimized PT-CT excited state (${}^1\pi\pi^*(CT)^{OPT}$) in the gas phase ($\epsilon = 1$). For clarity other transitions are not shown. For details see Figures 5 and 6 and Table 4.

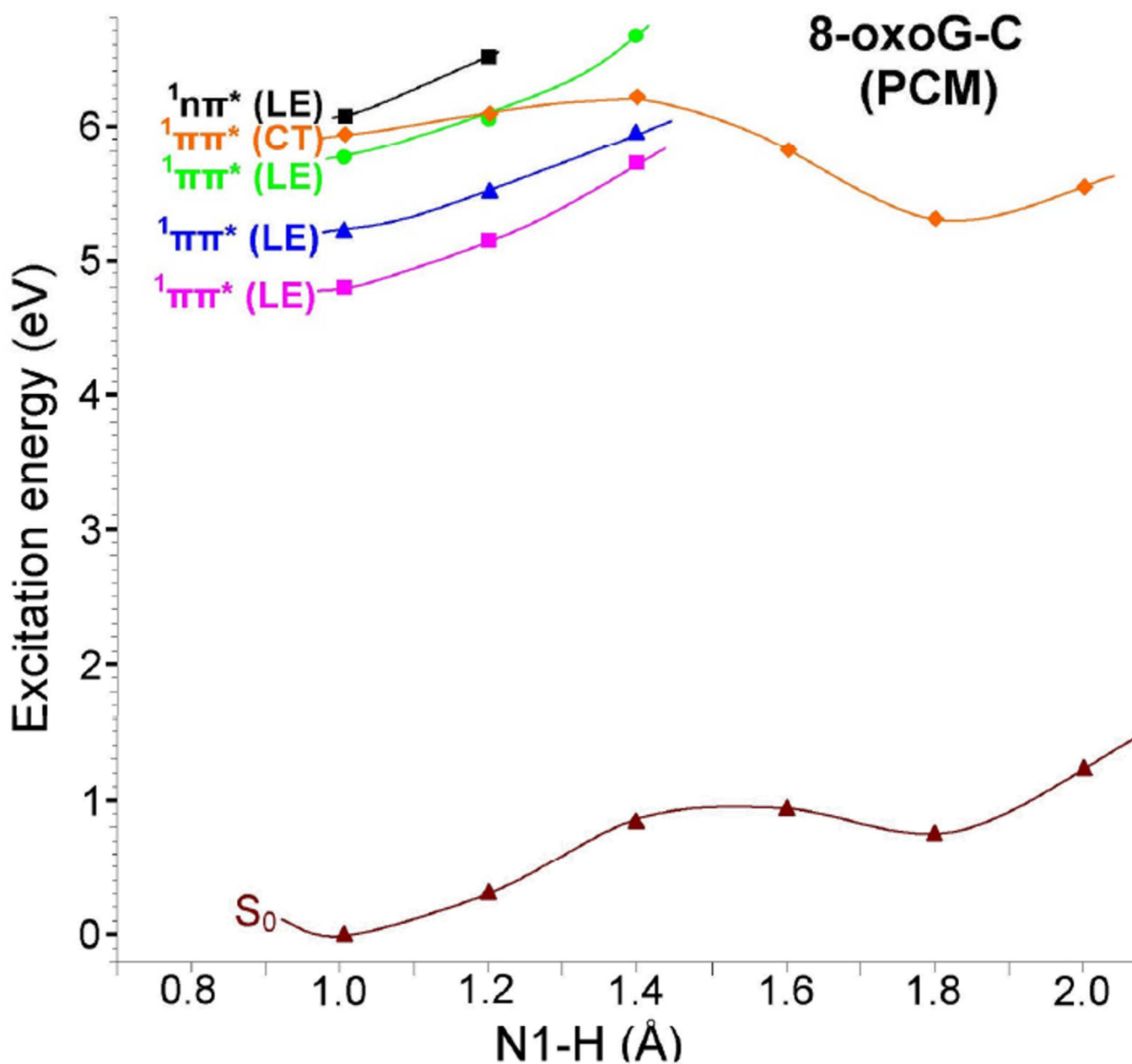


Figure 8. Vertical potential energy surface (PES) profile of the ground (S_0), $^1\pi\pi^*$ (LE), $^1n\pi^*$ (LE) and the lowest $^1\pi\pi^*$ (CT) excited states of 8-oxoG-C base pair calculated using the PCM-TD- ω B97XD/6-31G* method in water solution ($\epsilon = 78.4$) considering N1-H of 8-oxoG as a reaction coordinate. All the energies were calculated using the energy of the optimized ground state of 8-oxoG-C base pair as reference.

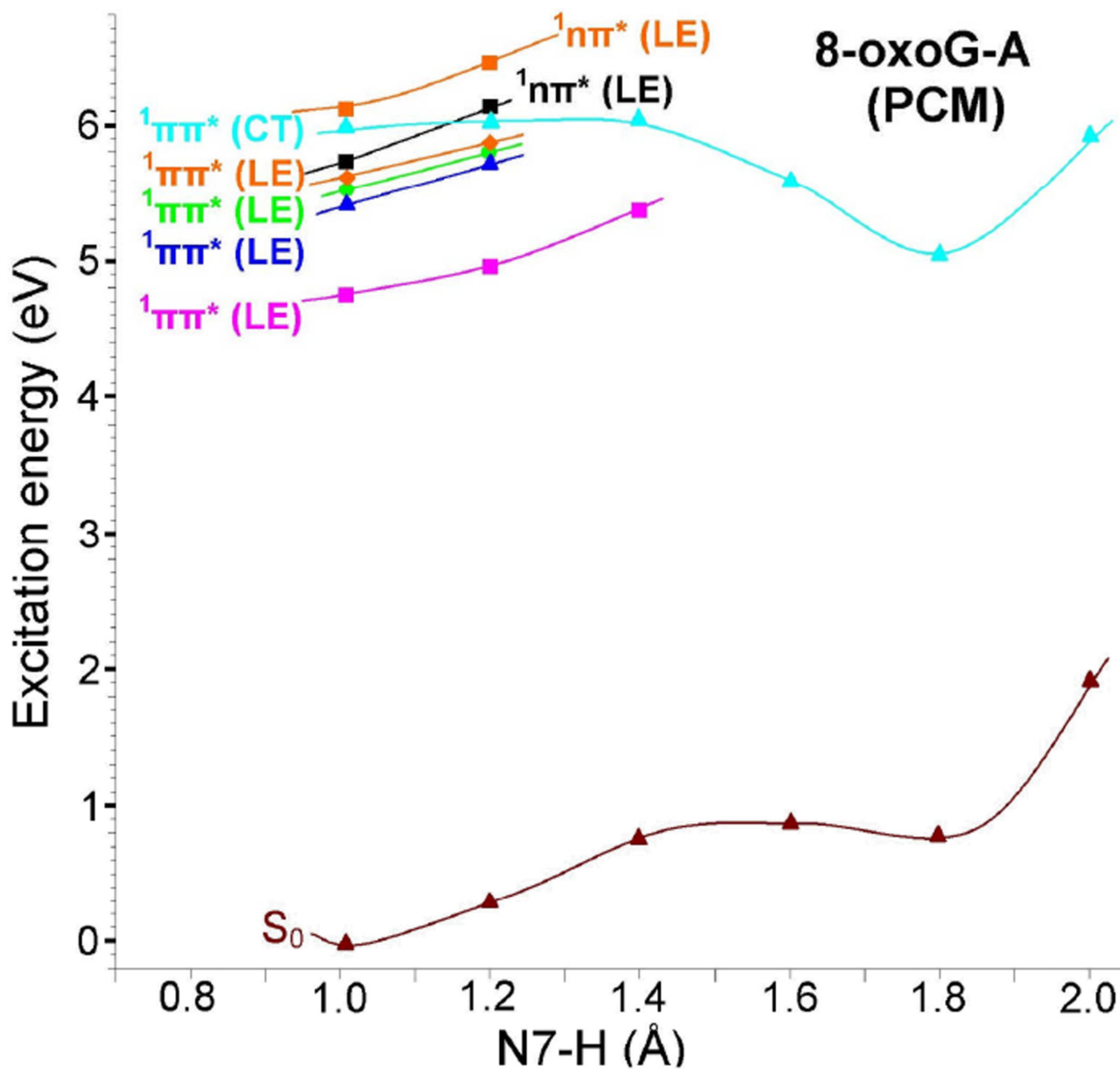


Figure 9.

Vertical potential energy surface (PES) profile of the ground (S_0), $1\pi\pi^*$ (LE), $1n\pi^*$ (LE) and the lowest $1\pi\pi^*$ (CT) excited states of 8-oxoG-A base pair calculated using the PCM-TD- ω B97XD/6-31G* method in water solution ($\epsilon = 78.4$) considering N7-H of 8-oxoG as a reaction coordinate. All the energies were calculated using the energy of the optimized ground state of 8-oxoG-A base pair as reference.

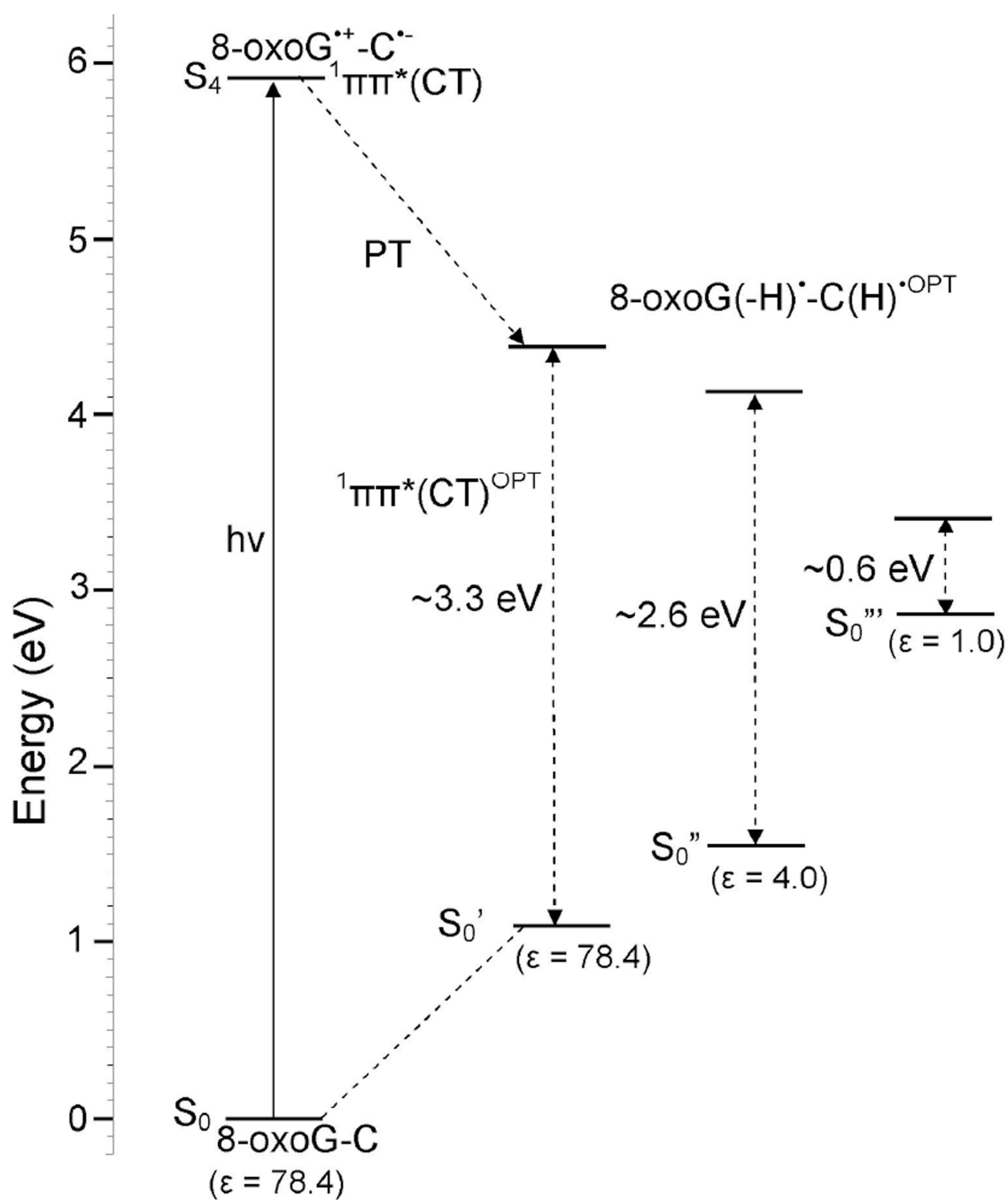


Figure 10.

Energy level diagram of $^1\pi\pi^*(CT)$ excited states of 8-oxoG-C base pair along with the optimized PT-CT excited state ($^1\pi\pi^*(CT)^{OPT}$) in $\epsilon = 78.4$ (water); 4.0 (DNA) and 1.0 (gas phase). For details see Figure 8 and Table 5. Calculations were done using the PCM-TD- ω B97XD/6-31G* method.

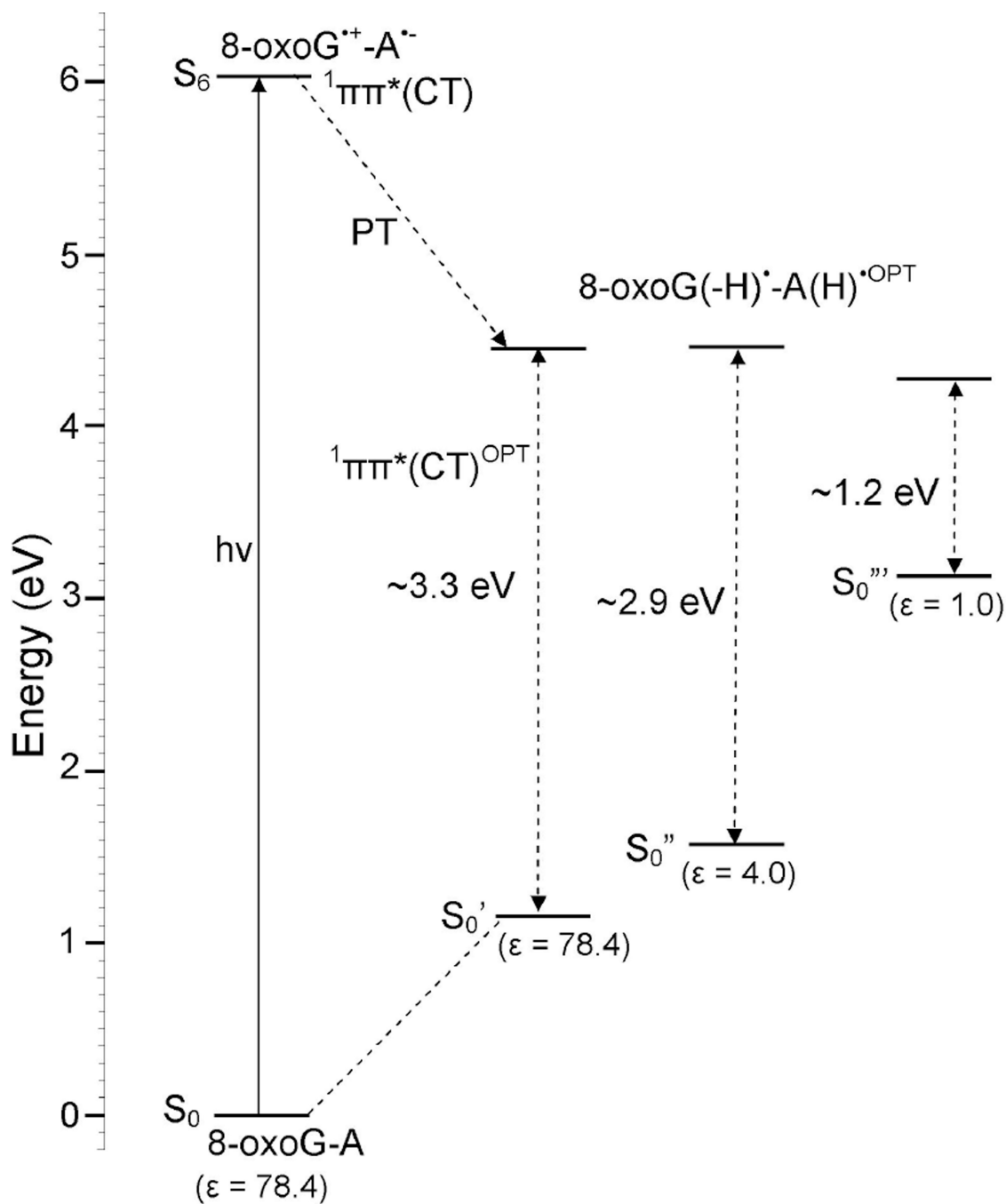


Figure 11.

Energy level diagram of $^1\pi\pi^*(CT)$ excited states of 8-oxoG-A base pair along with the optimized PT-CT excited state ($^1\pi\pi^*(CT)^{OPT}$) in $\epsilon = 78.4$ (water); 4.0 (DNA) and 1.0 (gas phase). For details see Figure 8 and Table 5. Calculations were done using the PCM-TD- ω B97XD/6-31G* method.

Table 1

Comparison of Methods: Vertical low-lying singlet excited state energies (E) in eV and oscillator strength (f) of G-C base pair calculated with the CC2/TZVP and ω B97XD/6-31G* methods ($\epsilon = 1$).

G-C base pair				
State	CC2/TZVP ^a		ω B97XD/6-31G* ^b	
	Transition	E(f)	Transition	E (f)
S ₁	G(π) \rightarrow G(π^*)	4.88 (0.061)	G(π) \rightarrow G(π^*)	5.22 (0.0616)
S ₂	C(π) \rightarrow C(π^*)	5.06 (0.063)	C(π) \rightarrow C(π^*)	5.32 (0.1036)
S ₃	G(π) \rightarrow C(π^*) (CT) ^c	5.23 (0.028)	G(π) \rightarrow C(π^*) (CT) ^c	5.45 (0.0114)
S ₄	C(n) \rightarrow C(π^*)	5.49 (0.001)	C(n) \rightarrow C(π^*)	5.72 (0.0010)
S ₅	C(π) \rightarrow C(π^*)	5.50 (0.183)	C(π) \rightarrow C(π^*)	5.92 (0.1238) S ₆ ^d
S ₆	G(π) \rightarrow G(π^*)	5.51 (0.425)	G(π) \rightarrow G(π^*)	5.75 (0.4124) (S ₅) ^d
S ₇	C(n) \rightarrow C(π^*)	5.80 (0.000)	C(n) \rightarrow C(π^*)	6.45 (0.0001) (S ₈) ^d
S ₈	G(n) \rightarrow G(π^*)	5.90 (0.000)	G(n) \rightarrow G(π^*)	5.94 (0.0005) (S ₇) ^d

^aRef. 35.

^bPresent work.

^cCharge transfer.

^dTransition.

Table 2

Comparison of Methods: Vertical low-lying singlet excited state energies (E) in eV and oscillator strength (f) of A-T base pair calculated with the CC2/TZVP and ω B97XD/6-31G* methods ($\epsilon = 1$).

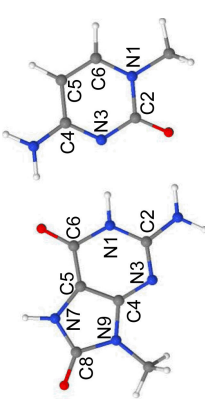
State	A-T base pair			
	CC2/TZVP ^a		ω B97XD /6-31G* ^b	
	Transition	E	Transition	E (f)
S1	T(n) \rightarrow T(π^*)	4.94	T(n) \rightarrow T(π^*)	5.33 (0.0001)
S2	T(π) \rightarrow T(π^*)	5.21	T(π) \rightarrow T(π^*)	5.41 (0.1777)
S3	A(π) \rightarrow A(π^*)	5.40	A(π) \rightarrow A(π^*)	5.51 (0.1132)
S4	A(π) \rightarrow A(π^*)	5.47	A(π) \rightarrow A(π^*)	5.57 (0.1947)
S5	A(n) \rightarrow A(π^*)	5.54	A(n) \rightarrow A(π^*)	5.63 (0.0003)
S6	-	-	A(n) \rightarrow A(π^*)	6.11 (0.0001)
S7	A(π) \rightarrow T(π^*)	6.04	A(π) \rightarrow T(π^*)	6.32 (0.0034)

^aRef. 36.

^bPresent calculation.

Table 3

Vertical lowest lying singlet excited state energies (E) in eV and oscillator strengths (f) of 8-oxoG-C base pair calculated using the TD-ωB97XD/6-31G* method (ε = 1).

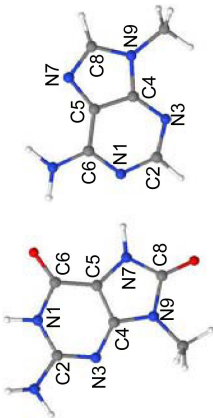


State	Transition	E (eV)	f	Configuration	Nature ^d
S ₁	8-oxoG(π) → 8-oxoG(π*)	4.79	0.1233	~35%	LE
S ₂	8-oxoG(π) → C(π*)	5.17	0.0348	~40%	CT
S ₃	C(π) → C(π*)	5.26	0.1153	~38%	LE
S ₄	8-oxoG(π) → 8-oxoG(π*)	5.78	0.3145	~46%	LE
S ₅	C(n) → C(π*)	5.81	0.0009	~21%	LE
S ₆	C, 8-oxoG(π) → C(π*)	5.91	0.1067	~40%; delocalized on C and 8OG	LE
S ₇	8-oxoG(n) → 8-oxoG(π*)	6.19	0.0001	~19%	LE

^dLE= local excitation; CT= charge transfer.

Table 4

Vertical lowest lying singlet excited state energies (E) in eV and oscillator strength (f) of 8-oxoG-A base pair calculated using the TD- ω B97XD/6-31G* method ($\epsilon = 1$)



State	Transition	E (eV)	f	Configuration	Nature ^d
S ₁	8-oxoG(π) \rightarrow 8-oxoG(π^*)	4.61	0.2128	~48%	LE
S ₂	8-oxoG(π) \rightarrow 8-oxoG(π^*)	5.44	0.0936	~38%	LE
S ₃	A(π) \rightarrow A(π^*)	5.47	0.2110	~41%	LE
S ₄	A(π) \rightarrow A(π^*)	5.57	0.2097	~33%	LE
S ₅	A(n) \rightarrow A(π^*)	5.66	0.0002	~40%	LE
S ₆	A, 8-oxoG(n) \rightarrow 8-oxoG(π^*)	6.04	0.0003	~21%; delocalized on 8-oxoG and A	LE
S ₇	8-oxoG(π) \rightarrow A(π^*)	6.16	0.0016	~48%	CT
S ₈	A(n) \rightarrow A(π^*)	6.19	0.0001	~41%	LE
S ₉	8-oxoG(π) \rightarrow 8-oxoG(π^*)	6.56	0.2895	~38%	LE

^a LE= local excitation; CT= charge transfer.

Table 5

Vertical lowest lying singlet excited state energies (E) in eV and oscillator strength (f) of 8-oxoG-C and 8-oxoG-C base pairs in solution ($\epsilon = 78.4$) calculated using the PCM-TD- ω B97XD/6-31G* method.

8-oxoG-C					
State	Transition	E (eV)	f	Configuration	Nature ^a
S ₁	8-oxoG(π) \rightarrow 8-oxoG(π^*)	4.80	0.1570	~46%	LE
S ₂	C(π) \rightarrow C(π^*)	5.22	0.2096	~44%	LE
S ₃	8-oxoG(π) \rightarrow 8-oxoG(π^*)	5.76	0.4277	~44%	LE
S ₄	8-oxoG(π) \rightarrow C(π^*)	5.93	0.0012	~47%	CT
S ₅	8-oxoG(n), C(π) \rightarrow C(π^*)	6.05	0.0396	~25%; delocalized on 8-oxoG and C	LE
8-oxoG-A					
S ₁	8-oxoG(π) \rightarrow 8-oxoG(π^*)	4.73	0.2531	~43%	LE
S ₂	A(π) \rightarrow A(π^*)	5.42	0.2498	~29%	LE
S ₃	A(π) \rightarrow A(π^*)	5.47	0.0688	~24%	LE
S ₄	8-oxoG(π) \rightarrow 8-oxoG(π^*)	5.62	0.3621	~45%	LE
S ₅	A(n) \rightarrow A(π^*)	5.71	0.0004	~36%	LE
S ₆	8-oxoG(π) \rightarrow A(π^*)	6.03	0.0011	~43%	CT
S ₇	8-oxoG(n) \rightarrow 8-oxoG(π^*)	6.12	0.0001	~24%	LE

^a LE= local excitation; CT= charge transfer.